ELSEVIER

www.elsevier.nl/locate/jelechem

Journal of Electroanalytical Chemistry 477 (1999) 97–110

JOURNAL OF ELECTROANALYTICAL CHEMISTRY

A model for the liquid feed direct methanol fuel cell

K. Scott [a,*], P. Argyropoulos [a], K. Sundmacher [b]

[a] *Department of Chemical and Process Engineering, University of Newcastle upon Tyne, Newcastle upon Tyne NE1 7RU, UK*
[b] *Max-Planck-Institut fur Dynamik komplexer technischer Systeme, D-39120 Magdeburg, Germany*

Received 23 April 1999; received in revised form 17 June 1999; accepted 6 August 1999

Abstract

Mass transport is a factor which limits the performance of solid polymer electrolyte fuel cells operating at relatively high current densities. The direct methanol solid polymer electrolyte fuel cell, unlike the hydrogen cell, suffers from mass transport limitations predominantly at the anode. In the liquid feed cell the mass transport limitations arise from diffusion of methanol in the carbon cloth covering the active electrocatalyst layer and from hydrodynamic limitations in the anode flow channel. A model of the methanol mass transport processes is presented which is used to predict the effective methanol concentration at the catalyst surface and thereby the anode polarisation. This model, together with an empirical model of the open circuit voltage and the cathode overpotential model, is used to predict the overall cell voltage, current density response of the fuel cell.

Keywords: Direct methanol fuel cell; Mass transport; Methanol crossover; Model

1. Introduction

Proton-exchange membrane fuel cells (PEMFC) are possible alternative power sources for stationary and mobile applications and electric vehicles. Methanol is a liquid fuel that has substantial electroactivity and can be oxidized directly to carbon dioxide and water on catalytically active anodes in a direct methanol fuel cell (DMFC). The direct methanol fuel cell, based on a solid polymer electrolyte (SPE) in the form of a proton conducting membrane, has the attraction of no liquid acidic or alkaline electrolyte. The structure of the DMFC is a composite of two porous electrocatalytic electrodes on either side of a solid polymer electrolyte membrane. In the DMFC, platinum alone is not a sufficiently active methanol oxidation electrocatalyst and the promotion of methanol oxidation has been actively studied. Significant results have been achieved with the use of binary catalysts, notably Pt–Ru. With these catalysts the second metal forms a surface oxide in the potential range for methanol oxidation [1]. Recent developments in electrode fabrication techniques and better cell designs have brought dramatic improvements in cell performance in small-scale DMFCs [1–11].

To date an essential condition for the high performance of a DMFC is the use of low concentrations of methanol. At concentrations higher than approximately 2 mol dm^{-3}, the cell voltage declines significantly due to permeation of methanol through the SPE (Nafion®) membrane, i.e. methanol crossover. This permeation results in a mixed potential at the cathode with a significant loss in oxygen reduction performance and also poor fuel utilisation. Thus an important area to improve the DMFC performance is in polymer membrane electrolytes to reduce methanol crossover.

Several researchers have reported limiting current densities for methanol oxidation [5,12]. Kaurenan and Skou [12] attributed this limiting current behaviour to saturation coverage of adsorbed OH on the platinum surface. Observed limiting currents on platinum supported catalysts occur at potentials of approximately 0.65 V (vs. RHE) where the fractional coverage of OH is 0.5, as predicted by a Langmuir isotherm. Measurements of methanol oxidation using linear sweep voltammetry, at 5 mV s^{-1}, on platinum rotating discs by Chu and Gilman [13] show a definite hydrodynamic

* Corresponding author. Tel.: +44-191-2228771; fax: +44-191-2225292.
E-mail address: k.scott@ncl.ac.uk (K. Scott)

0022-0728/99/$ - see front matter
PII: S0022-0728(99)00359-9

influence. Peak methanol oxidation currents (measured in 0.5 M H_2SO_4 and 1.0 M methanol) at approximately 0.75 V (vs. RHE) decrease with increasing rotation rate. Ravikumar and Shukla [5] have reported data for the DMFC using carbon supported platinum–ruthenium catalysts for methanol oxidation. Limiting current densities are obtained, at 0.5–1.0 M methanol concentrations, which are approximately proportional to the methanol concentration. Noticeably the limiting current densities observed by Ravikumar and Shukla [5] are very much lower, at equivalent methanol concentrations, than those of Kaurenan and Skou [12]. The electrode structures used were significantly different. Kaurenan and Skou used a 50 μm thick anode layer, (40 wt% Pt on Vulcan XL-72R) with a Pt loading of 1.0 mg Pt cm^{-2}, Ravikumar and Shukla used a catalyst layer made from Pt–Ru supported onto Ketjen black with a loading of 5 mg cm^{-2} of catalyst; which was covered with a carbon cloth 'diffusion layer', 0.3 mm thick.

Previous models of the DMFC have been few. Verbrugge describes a simple diffusion model of methanol through a PEM, assuming dilute solution theory [14]. Validation of the model with experimental data showed that the diffusion rate of methanol through the membrane was nearly as fast as through water. A second model of methanol transfer, by diffusion and electroosmosis, across a PEM has been used to explain observed experimental data for a vapour feed DMFC [15]. This model has been extended to include a one dimensional model of the potential distribution and concentration distribution of methanol in the anode electrocatalyst layer for a vapour feed system [2,16]. The model gives good agreement with experimental data except under conditions where mass transport becomes rate limiting. Very recently, Baxter et al. [17] have presented a model of the DMFC anode which is considered to be a porous electrode consisting of an electronically conducting catalyst structure that is thinly coated with an ion selective polymer electrolyte. The pores of the electrode are filled with aqueous methanol solution in which all species of the reaction are free to transport. Mass transfer in the anode is defined in terms of a pseudo-mass-transport coefficient. The model is however not validated against experimental data and does not consider mass transport of species in other regions of the electrode assembly.

The purpose of this paper is to report a model for the DMFC which accounts for the influence of methanol and water mass transport, and of carbon dioxide gas flow, on performance. The model considers the hydrodynamic influence in the flow channel associated with carbon dioxide gas evolution, methanol mass transport in the membrane electrode assembly (MEA), diffusion layers and methanol transport across the membrane. The model also incorporates a semi-empirical model for the open circuit potential in the presence of methanol crossover. Experimental data are used to validate various aspects of the mass transfer behaviour of the anode and cell polarisation data.

2. DMFC anode mass transport

Mass transport limitations in the anode of liquid feed DMFC, shown schematically in Fig. 1, can potentially arise in several ways:

1. at the catalyst sites which are covered in water and at which carbon dioxide is formed;
2. in the Teflon/Nafion® loaded carbon gas diffusion layer;
3. in the carbon cloth backing layer;
4. at the surface of the carbon cloth backing layer where the gas bubbles are released into the flowing methanol solution.

Carbon dioxide gas will be generated in the anode structure at a position dependent upon local conditions of pressure, temperature, carbon dioxide solubility and bubble nucleation. Due to the moderate solubility of carbon dioxide in the aqueous methanol solution, bubble generation will occur away from the thin anode

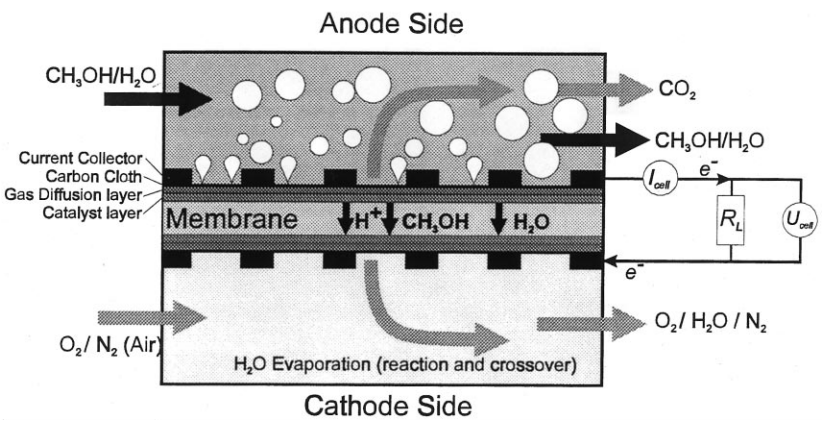

Fig. 1. Schematic diagram of the direct methanol fuel cell.

catalyst surface. In practice, methanol solution is recycled to the cell from a reservoir and thus will contain a significant amount of dissolved carbon dioxide. Thus it is likely, and is assumed here, that gas bubbles will be formed in the diffusion layer and flow counter-current to the mass transport of liquid.

The combined effect of the above mass transfer effects, assuming all processes are linear with respect to methanol concentration, gives the overall 'effective' mass transfer coefficient, k_{eff}, as

$$1/k_{eff} = 1/k_l + 1/k_{cl} + 1/k_c + 1/\xi k^* \quad (1)$$

when k_l is the hydrodynamic mass transport coefficient, k_{cl} is the carbon cloth mass transport coefficient, k_c is the carbon gas diffusion layer mass transport coefficient and ξk^* is the effective electrochemical methanol oxidation rate constant in the catalyst layer, where, ξ, is an effectiveness factor for the catalyst.

Diffusion mass transfer in the cloth depends upon the liquid void fraction and the cloth pore structure and can be represented by

$$j = nFk^\circ_{cl}\, e_c^m \Delta c_{c1} \quad (2)$$

where Δc_{c1} is the concentration change over the cloth thickness, e_c is the liquid voidage, m is an empirical parameter which allows for cloth tortuosity and porosity, and $k^\circ_c = D_{MeOH}/l_{cl}$ where l_{cl} is the cloth thickness.

The diffusion coefficient of methanol in water D_{MeOH} is estimated to be 2.8×10^{-9} m^2 s^{-1} [18]. The carbon cloth thickness varied between 140 and 280 μm. Taking a thickness of 280 μm, and assuming mass transfer through a stationary methanol solution, the mass transfer coefficient for a cloth of 100% porosity is approximately 10^{-5} m s^{-1}.

Such a mass transport coefficient places a potentially large restriction on the performance of the DMFC and clearly indicates the need for both effective electrode design and suitable mass transport analysis. In practical operation the carbon cloth (or paper) is partly filled with carbon dioxide gas and the available liquid voidage is therefore lower than that of the cloth voidage. The estimation of the actual liquid voidage (or liquid saturation s_l,), is therefore essential to satisfactory model the mass transport process. For this model, capillary pressure theory is a reasonable approach [19]. Appendix A provides a macroscopic model, based on momentum balances of the two phase flow of aqueous methanol solution and carbon dioxide gas in a porous media, for estimation of the liquid voidage as a function of current density.

An alternative simplified model is to assume that the carbon dioxide gas is evolved as a bubble swarm into a stationary liquid and that the voidage of gas is determined from the rise velocity of the gas bubble swarm. This rise velocity can be estimated simply from Richardson and Zaki drag coefficient correlations [20]. The volumetric production of CO_2 is governed by the following relationship, if ideal gas behaviour is assumed:

$$V_g = \frac{RT}{P}\frac{j}{6F} \quad (3)$$

and it is therefore directly dependent on the current density.

This model clearly ignores the influence of the drag of the carbon cloth, but could be applicable to horizontally positioned electrodes in which the buoyancy of the gas assists movement of bubbles away from the surface.

In comparison to the carbon cloth, the carbon diffusion layer thickness is small, and thus this model largely ignores this contribution to the mass transport resistance. In principle both of the diffusion regions can be modelled as one effective overall resistance.

The value of k_l depends on the hydrodynamics in the channel as well as on gas bubble generation at the surface. Mass transfer at gas evolving electrodes has been measured for oxygen evolution [21] and chlorine evolution [22] at vertical electrodes. That data for oxygen evolution can be correlated, allowing for differences in gas evolution rates for oxygen evolution and carbon dioxide evolution with current density, as a function of current density, by the expression:

$$k_{av} = 1.87 \times 10^{-6}\,(j/3)^{0.32} \quad (4)$$

where k_{av} is the average mass transfer coefficient.

Overall the effect of increased current density on the mass transfer characteristics of carbon cloth based anodes in the DMFC may be a combined effect of:

- enhancement due to increased gas evolution at the cloth surface and
- suppression due to decreased liquid volume in the cloth.

In the case of the DMFC, gas evolves from the surface of a carbon cloth positioned well away from the active electrode region. This gas evolution is, as observed in flow visualisation studies [23], not uniformly distributed. Thus overall estimates of the influence of bubble generation and movement on mass transfer effects in the DMFC are approximate.

Experimental mass transfer coefficients, determined from measurement of limiting current densities [24], shown in Fig. 2, are in the range of approximately $2.5–6.0 \times 10^{-5}$ m s^{-1}. The trend shown in the data of the effect of methanol concentration, i.e. increased limiting current density, appears to be a combined effect of gas bubble mass transport enhancement and suppression of mass transport due to bubble accumulation in the carbon diffusion layers.

Using the steady state model, presented in Appendix A, the liquid voidage in the carbon cloth varies typically as shown in Fig. 3. The liquid saturation (and voidage) falls rapidly as the current density increases,

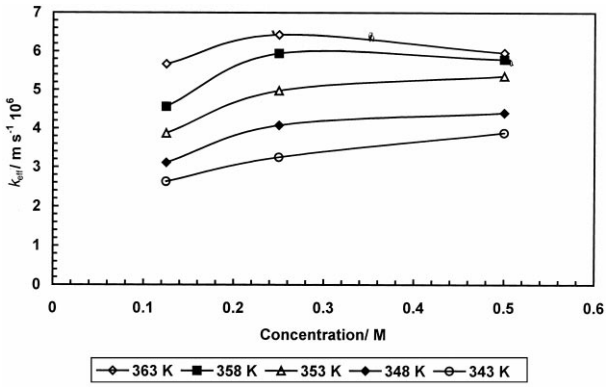

Fig. 2. Effective mass transfer coefficients for the direct methanol fuel cell determined at limiting current conditions.

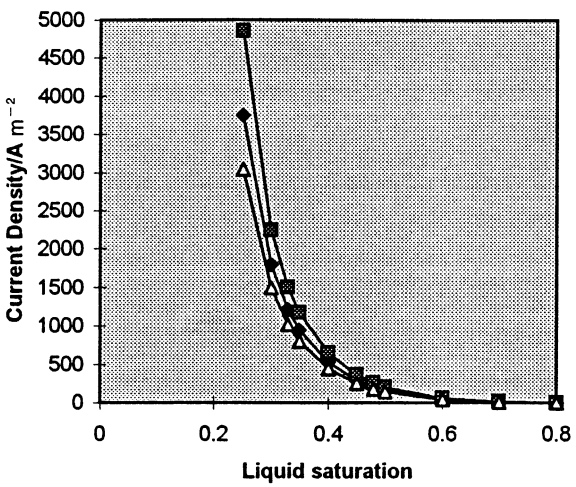

Fig. 3. Predicted liquid saturation in the carbon cloth from capillary pressure theory. (a) Variation of liquid saturation with current density. ◆, 70°C; ■, 80°C; △, 90°C.

Table 1
Parameters used in mass transfer model

Carbon cloth porosity	0.875
Carbon cloth thickness	140×10^{-6} m
Diffusivity of methanol at 70°C	2.8×10^{-9} m^2 s^{-1}
Viscosity of water	0.41 (70°C), 0.355 (80°C), 0.318 (90°C)
Viscosity of CO_2	0.162 (70°C), 0.17 (80°C), 0.175 (90°C)
Nafion® 117 conductivity	0.01 S cm^{-1}
Methanol reaction order, n	0.5
Methanol transfer coefficient	1.0
Oxygen cathode transfer coefficient	0.6

due to the increase in gas evolved at the anode. The variation of liquid saturation also depends on the temperature of operation due to, predominantly, the variation in viscosity of gas and liquid. At a fixed current density the liquid saturation increases with decreasing temperature. The spatial variation of liquid voidage in the cloth, as computed from the capillary pressure model, is typically within 10% of that predicted by the steady state model.

The variation of the cloth mass transfer coefficient with increase in current density reflects the decrease in liquid phase voidage. The combined mass transfer effects produce a variation of overall mass transport coefficient with current density, using the parameters in Table 1, which exhibits a broad maximum (Fig. 4a). Fig. 4b, shows the variation in mass transfer coefficient with methanol concentration. This concentration is that which gives the limiting current in the DMFC, i.e. with the carbon dioxide evolution rate at it maximum, limiting, value. These data are therefore determined under conditions identical with values determined experimentally, shown in Fig. 2. Agreement between the model prediction and experimental data is reasonable, considering the uncertainty in predicted mass transfer coefficient in the channel.

3. Theoretical model

There are generally two important mass transfer restrictions in the direct methanol fuel cell; one due to the construction of the MEA and the second arising from CO_2 production in the anodic oxidation of methanol

$$CH_3OH + H_2O \rightarrow 6\ e^- + 6\ H^+ + CO_2 \quad (5)$$

The MEA is constructed as a sandwich of carbon cloth, gas diffusion layer, anode electrocatalyst layer, membrane, cathode electrocatalyst layer, gas diffusion layer, and carbon cloth. Due to diffusion and electroosmosis, there is a constant convection of water through the MEA from the anode to the cathode side. It can therefore be assumed that the electrode is flooded. However, as the feed solution is a dilute methanol solution, methanol transfer to the cell can be limited by the obstructions posed by the MEA.

It is the objective of this model to determine the effective concentration of methanol at the diffusion-layer | anode interface. The model considers the anode catalyst layer to be pseudo one-dimensional and that the carbon cloth and gas diffusion layer structure of the MEA are to be treated as a unit, posing a major mass transfer resistance. Although the carbon cloth is highly porous, it is typically rendered partially hydrophobic to facilitate removal of carbon dioxide gas. Both the hydrophobicity and the generation of gas restrict the mass transfer of methanol in the aqueous solution through the carbon cloth. This model is based on several assumptions:

- the fuel cell is operated isothermally;
- there is no pressure difference between the compartments;

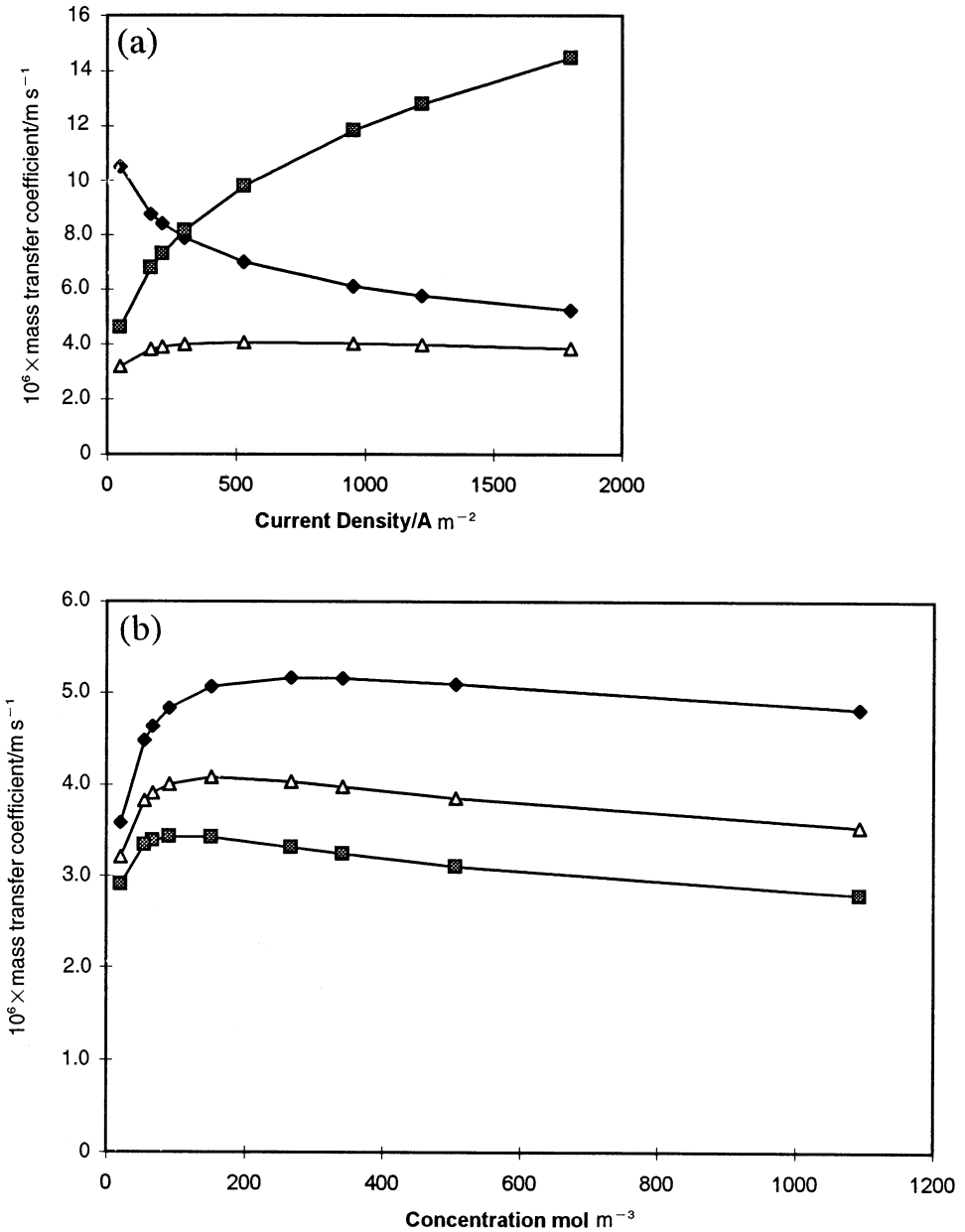

Fig. 4. Predicted variation of anode side mass transfer coefficient. (a) Variation of mass transfer coefficient with current density. ◆, cloth; ■, channel; △, overall. (b) Variation of overall mass transfer coefficient with concentration ■, 70°C; △, 80°C; ◆, 90°C.

- the cathode side reaction is not rate limiting;
- the anode side is treated as pseudo-one-dimensional;
- the concentration of methanol in the anode channel is defined as the feed concentration. Under the assumption that the flow channel is a well mixed system, this concentration is in fact the exit concentration of the cell. However, even at limiting currents of 100 mA cm^{-2} and at low concentrations, e.g. 0.25 M, the variation in flow channel concentration is small.
- transfer of water across the membrane is by diffusion and electroosmosis;
- mass transfer of methanol in the carbon diffusion layer is defined in terms of an effective diffusion coefficient, discussed in Section 2;
- the anode is assumed to be a pseudo one dimensional surface;
- the change in surface tension of the aqueous solution with change is methanol concentration is negligible as the liquid in predominantly water.

4. General relationship between concentration and mass transfer

Fig. 5 shows the model of the anode which includes transport processes associated with the cation exchange

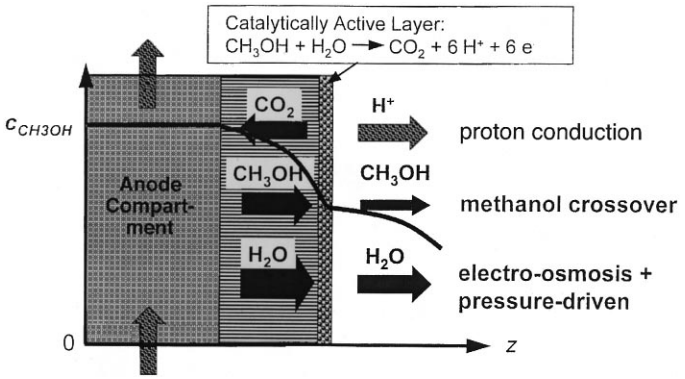

Fig. 5. Schematic model of the DMFC anode.

membrane. Methanol transfer flux in the MEA is brought about by reaction at the anode, N_a, and transfer across the membrane N_{ME}.

The reaction flux is

$$N_a = j/6F \tag{6}$$

The methanol flux through the carbon cloth is a combination of diffusion N_{diff} and convection expressed as

$$N'_{MeOH} = N_{Diff} + x_{Me}N_T \tag{7}$$

where x_{Me} is the local methanol mol fraction and N_T is the total flow of water and methanol. As the methanol concentration is low, the total flow is approximately the flow of water only, i.e.

$$N_T = N_{H_2O} \tag{8}$$

For dilute methanol solution used in the DMFC the local mol fraction can be approximated by

$$x_{Me} = \frac{c_{MeOH}}{c_{H_2O} + c_{MeOH}} \overset{c_{H_2O} >> c_{MeOH}}{\approx} \frac{c_{MeOH}}{c_{H_2O}} = \frac{18c_{MeOH}}{\zeta_{H_2O}} \tag{9}$$

where c is the concentration and, ζ_{H_2O} is the density of water.

The diffusion flux of methanol is given by Fick's Law:

$$N_{Diff} = -D_e \frac{dc_{MeOH}}{dx} \tag{10}$$

where D_e is the effective diffusion coefficient of methanol.

Combining Eq. (7) to Eq. (10) and solving

$$\ln\left[\frac{c^a_{MeOH} - \frac{\zeta_{H_2O}N'_{MeOH}}{18N'_{H_2O}}}{c^f_{MeOH} - \frac{\zeta_{H_2O}N'_{MeOH}}{18N'_{H_2O}}}\right] = \frac{1}{k^*_c}\frac{18N'_{H_2O}}{\zeta_{H_2O}} \tag{11}$$

where, $k^*_c = D_c/l_a$, is the effective mass transfer coefficient in the carbon cloth and diffusion layers, and superscripts a and f refer to anode and feed concentrations, respectively.

5. Water transport

The water transport through the cloth is caused by three different factors:

1. the water required for the anode Eq. (6)
2. the electroosmotic water transfer through the membrane with H^+ ions

$$N_{drag} = \lambda_{H_2O} j/F \tag{12}$$

3. diffusion across the membrane

$$N_{Diff} = (D^m_{H_2O}/l_m)(c^a_{H_2O} - c^c_{H_2O}) \tag{13}$$

where $D^m_{H_2O}$ is the diffusion coefficient of the water in the membrane, $c^a_{H_2O}$ and $c^c_{H_2O}$ are the water concentrations on the anode and cathode side, respectively. Strictly, the driving force for water diffusion should be expressed in terms of water activity.

The water transfer across the membrane is influenced by the evaporation of water into the cathode gas stream and the production of water by the cathode reaction. Both these factors will vary the effective water activity or concentration at the cathode side. In addition, methanol crossover from anode to cathode will modify the cathode side water concentration through its partial oxidation at the cathode. At this point it is appropriate to consider experimental data on water transfer as given, for example, by Ren et al. [25]. Water transfer starts at a finite value at zero current density and rises relatively slowly with current density until a 'critical current density' (j_{crit}) is reached, after which the water transfer increases linearly with current density. At $j = 0$, the water transfer is due to diffusion through the membrane, which in turn is influenced by the cathode side pressure and temperature. As load is applied to the cell, water accumulates in the cathode pores and the activity of the water effectively increases. This continues until the anode and cathode side water concentrations (or activities) are equal, after which the water transfer is by electroosmotic drag. This is shown graphically in Fig. 6.

As an approximation, at a constant evaporation rate, we assume that the cathode accumulation of water varies linearly with current density in the following form:

$$c^c_{H_2O} = c^c_{H_2O}|_{j=o} + \gamma j \tag{14}$$

In this equation, γ, is an experimentally determined constant.

The water transfer across the membrane is expressed simply as

$$N_{H_2O} = N_{drag} + (D^m_{H_2O}/l_m)(c^a_{H_2O} - c^c_{H_2O}) \tag{15}$$

The water transfer at $j = 0$, is therefore

$$N_{H_2O}|_{j=0} = (D^m_{H_2O}/l_m)(c^a_{H_2O} - c^{c_{H_2O}}|_{j=0}) \tag{16}$$

Combining Eqs. (14) to (16), yields:

$$N_{H_2O} = N_{drag} + N_{H_2O}|_{j=0} - (D^m_{H_2O}/l_m)\gamma j \quad (17)$$

This applies up to a critical density, which is defined as

$$j = j_{crit} \quad \text{if} \quad N_{H_2O} = N_{drag} \quad (18)$$

It follows that

$$\frac{D^m_{H_2O}}{l_m}\gamma = \frac{N_{H_2O}|_{j=0}}{j_{crit}} \quad (19)$$

When the current density is higher than the critical current density,

$$N_{H_2O} = N_{drag} \quad \text{if} \quad j > j_{crit} \quad (20)$$

Finally, using Eqs. (6), (12) and (13) the total water transport across the membrane is given as:

$$N'_{H_2O} = N^a_{H_2O} + N_{H_2O} =$$

$$\begin{cases} \frac{j}{6F} + \frac{\lambda_{H_2O} j}{F} + N_{H_2O}\Big|_{j=0} - \frac{D^m_{H_2O}}{l_m}\gamma j & \text{if} \quad j < j_{crit} \\ \frac{j}{6F} + \frac{\lambda_{H_2O} j}{F} & \text{if} \quad j > j_{crit} \end{cases} \quad (21)$$

The general behaviour of this model of water transport is shown in Fig. 7, and water transport parameters are given in Table 2.

5.1. Methanol transport in the membrane

Methanol transport is by diffusion and by electroosmosis, with water, leading to

$$N_{Me} = \frac{\lambda_{Me} j}{F} + \frac{D^m_{Me}}{l_m}\Delta c^m_{Me} \quad (22)$$

where D^m_{Me} is the diffusion coefficient of methanol in the membrane, Δc^m_{Me} is the concentration difference of methanol across the membrane, which is approximately equal to c^a_{Me}, as the concentration of methanol at the cathode side is small, due to its oxidation and evaporation. N_{Me} is also denoted as the methanol crossover and, in principle, can be used to calculate mixed potentials.

The drag coefficient is assumed to be given by:

$$\lambda_{MeOH} = x^a_{MeOH}\lambda_{H_2O} = \frac{18 c^a_{MeOH}}{\zeta_{H_2O}}\lambda_{H_2O} \quad (23)$$

That is methanol in aqueous solution is dragged with the water in proportion to the mol fraction of methanol in solution. Combining Eqs. (6), (22), (23) and (4), the total methanol flow is expressed as:

$$N'_{MeOH} = \frac{j}{6F} + \frac{18}{\zeta_{H_2O} F}\lambda_{H_2O} c^a_{MeOH} j + \frac{D^m_{MeOH}}{l_m} c^a_{MeOH} \quad (24)$$

The above model equations are readily solved to determine the variation of methanol anode concentra-

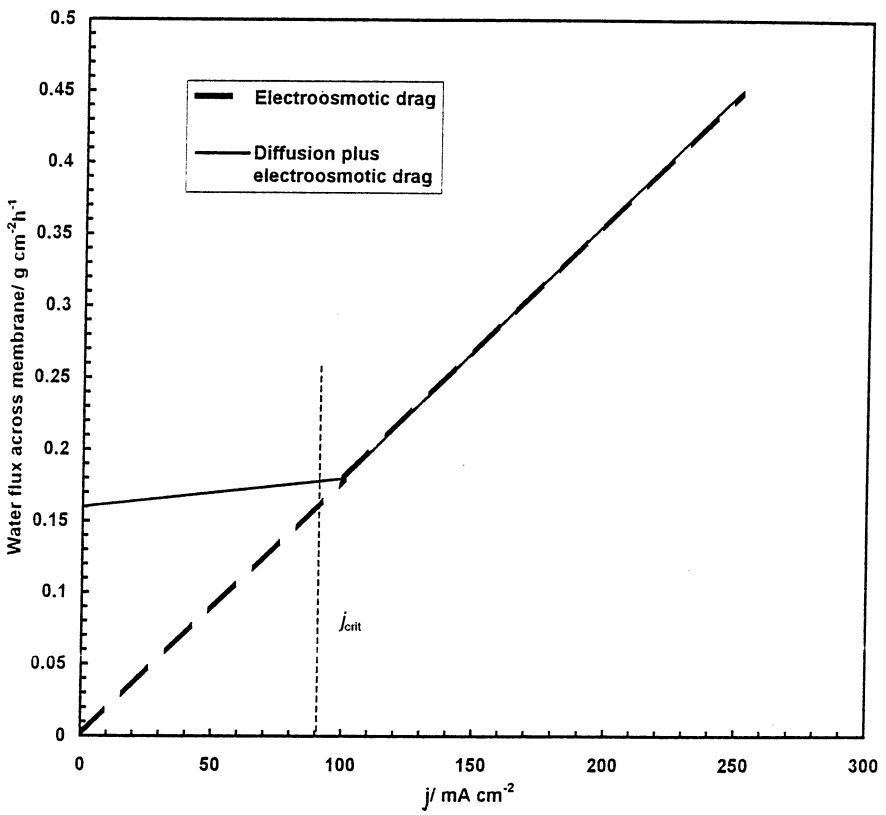

Fig. 6. Water transfer characteristics of Nafion® membrane.

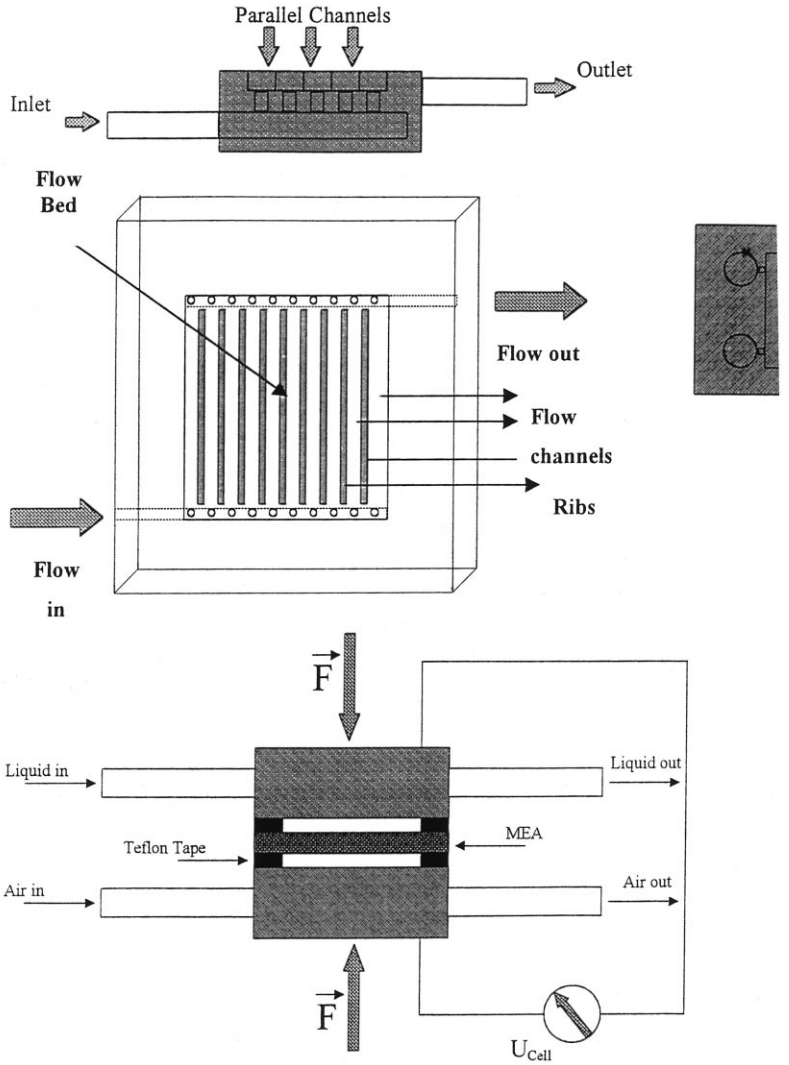

Fig. 7. Experimental direct methanol fuel cell.

tion with the current density as a function of the system parameters. The solution to the model depends upon the value of the current density in relation to the critical current density

5.2. ($j > j_{crit}$)

For $j > j_{\text{crit}}$, there is no influence of methanol diffusion. The anode interface concentration is given by:

$$c^{\text{a}}_{\text{MeOH}} = \frac{\exp\left(\frac{1}{k^{*}_{\text{c}}}\frac{A}{\zeta_{\text{H}_2\text{O}}}\right)\left(c^{\text{f}}_{\text{MeOH}} - \frac{C}{A}\right) + \frac{C}{A}}{1 - \frac{B}{A} + \frac{B}{A}\exp\left(\frac{1}{k^{*}_{\text{c}}}\frac{A}{\zeta_{\text{H}_2\text{O}}}\right)} \tag{25}$$

where

$$A = 18\left(\frac{j}{6F} + \frac{\lambda_{\text{H}_2\text{O}} j}{F}\right)$$

$$B = \frac{18}{F}\lambda_{\text{H}_2\text{O}} + \frac{\zeta_{\text{H}_2\text{O}} D^{\text{m}}_{\text{MeOH}}}{l_{\text{m}}}$$

$$C = \frac{\zeta_{\text{H}_2\text{O}} j}{6F}$$

5.3. ($j < j_{crit}$)

For $j < j_{\text{crit}}$, the anode interface concentration is given by

Table 2
Membrane water transport parameters determined from data of Ren et al. [25]

T/°C	P/bar	λ	$N_{\text{H}_2\text{O}}\|_{j=0}$/mol m^{-2} s^{-1}	j_{crit}/A m^{-2}
80	2.37	3.16	0.045262	1863.8
80	0.89	3.16	0.082731	2958.5
60	2.37	2.86	0.023843	913.8
60	0.89	2.86	0.047778	1818.9

$$c^{a}_{Me} = \frac{\exp\left(\frac{1}{k^{*}_{c}}\frac{D}{\zeta_{H_2O}}\right)\left(c^{f}_{MeOH} - \frac{C}{D}\right) + \frac{C}{D}}{1 - \frac{B}{D} + \frac{B}{D}\exp\left(\frac{1}{k^{*}_{e}}\frac{D}{\zeta_{H_2O}}\right)} \quad (26)$$

where

$$D = 18\left(\frac{j}{6F} + \frac{\lambda_{H_2O} j}{F} + N_{H_2O}|_{j=0} - \frac{D^{m}_{H_2O}}{l_m}\gamma j\right)$$

6. Experimental

Tests on the DMFC were performed with a cell, shown schematically in Fig. 6, with a cross-sectional area of 9 cm^2. The cell was fitted with one membrane electrode assembly sandwiched between two graphite blocks which had a flow bed, in the form of parallel channels, cut out for methanol and oxygen air flow. The cell was held together between two copper current collectors, two plastic insulation sheets and two stainless steel or aluminium backing plates using a set of retaining bolts positioned around the periphery of the cell. Electrical heaters, supplied by Watson Marlow, were placed behind each of the graphite blocks in order to heat the cell to the desired operating temperature. The graphite blocks were also provided with electrical contacts and small holes to accommodate thermocouples. The fuel cells were used in a simple flow rig which consisted of a Watson Marlow peristaltic pump to supply aqueous methanol solution, from a reservoir, to a Eurotherm temperature controller to heat the methanol. Air was supplied from cylinders, at ambient temperature, and the pressure regulated by pressure regulating valves. All connections between the cells and equipment were with PTFE tubing, fittings and valves

MEAs studied in this work were made in the following manner: the anode consisted of a Teflonised (20%) carbon cloth support (E-Tek, type 'A'), of 0.35 mm thickness, upon which was spread a thin (diffusion layer) layer of uncatalysed (Ketjenblack 600) carbon, bound with 10 wt% Nafion® from a solution of 5 wt% Nafion® dissolved in a mixture of water and lower aliphatic alcohols (Aldrich). The catalysed layer, consisting of 50 wt% Pt–Ru (2 mg cm^{-2} metal loading) dispersed on carbon (Ketjen) and bound with 10 wt% Nafion®, was spread on this diffusion backing layer. The catalyst content on the cathode was 1 mg cm^{-2}. Application of the thin layer of Nafion® bound uncatalysed carbon was found to improve the performance of the anode, probably by enabling greater access to active catalyst sites for methanol, water and protons. A thin layer of Nafion® solution was spread onto the surface of each electrode. Details of catalyst preparation are described elsewhere [11]. In brief, catalyst preparation used oxidation of colloidal Pt/Ru dispersions. This chemistry is based on soluble sulphito complexes of the form $Na_6Pt(SO_3)_4$ and $Na_4Ru(SO_3)_3$ and gives rise to 2 nm M–O particles adsorbed on the carbon. On chemical or electrochemical reduction, 2 nm particles of Pt, Ru or Pt–Ru are formed. The cathode was constructed using a similar method as for the anode, using a thin diffusion layer bound with 15 wt% PTFE, and 1 mg cm^{-2} Pt black (Johnson Matthey) with 10 wt% Nafion® in the catalyst layer. The electrodes were placed either side of a pre-treated Nafion® 117 membrane (Aldrich). This pre-treatment involved boiling the membrane for 1 h in 5 vol% H_2O_2 and 1 h in 1 mol dm^{-3} H_2SO_4 before washing in boiling Millipore water (>18 mΩ) for 2 h with regular changes of water. The assembly was hot-pressed at 100 kg cm^{-2} for 3 min at 135°C. The resulting MEA was installed in the cell after pressing, and hydrated with water circulated over the anode at 75°C for 48 h.

7. Cell voltage characteristics

7.1. Anode polarisation

For fuel cells the cell voltage is obtained from the combined effects of thermodynamics, kinetics, mass transport and ohmic resistance. For simplicity this voltage is frequency quoted as

$$V_{cell} = E + \eta_{act} + \eta_{ohmic}$$
$$= E_o - b\log j - RI + b\log j_o - b\log(c_b/c_s) \quad (27)$$

where b = Tafel slope, R is an internal resistance j_o is the exchange current density and the last term allows for mass transport limitation, i.e. the electrocatalyst surface concentration is lower than that in the 'bulk' electrolyte.

As a simple kinetic model for methanol oxidation, Tafel type kinetics are chosen

$$j = j_0 \frac{c^{a^n}_{MeOH}}{c^{f}_{MeOH}}\exp\left[\frac{\alpha F}{RT}(E - E^{\circ})\right] \quad (28)$$

where j_0 is the exchange current at the reference potential, α is the transfer coefficient and n is the order of reaction with respect to methanol concentration.

Re-arranging gives the overpotential:

$$(E - E^{\circ}) = \frac{RT}{\alpha F}\left[\ln\frac{j}{c^{a^n}_{MeOH}} - \ln\frac{j_0}{c^{f}_{MeOH}}\right] \quad (29)$$

The effect of temperature on the open circuit voltage is given by

$$E = E^{\circ} + \Delta T\left(\frac{\partial E}{\partial T}\right) \quad (30)$$

where $E^{\circ} = 1.216$ V at $T = 298$ K and $(\partial E/\partial T)$has been identified over the temperature range as $(\partial E/\partial T) = -0.14$ mV K^{-1} and $\Delta T = T - 298$ K.

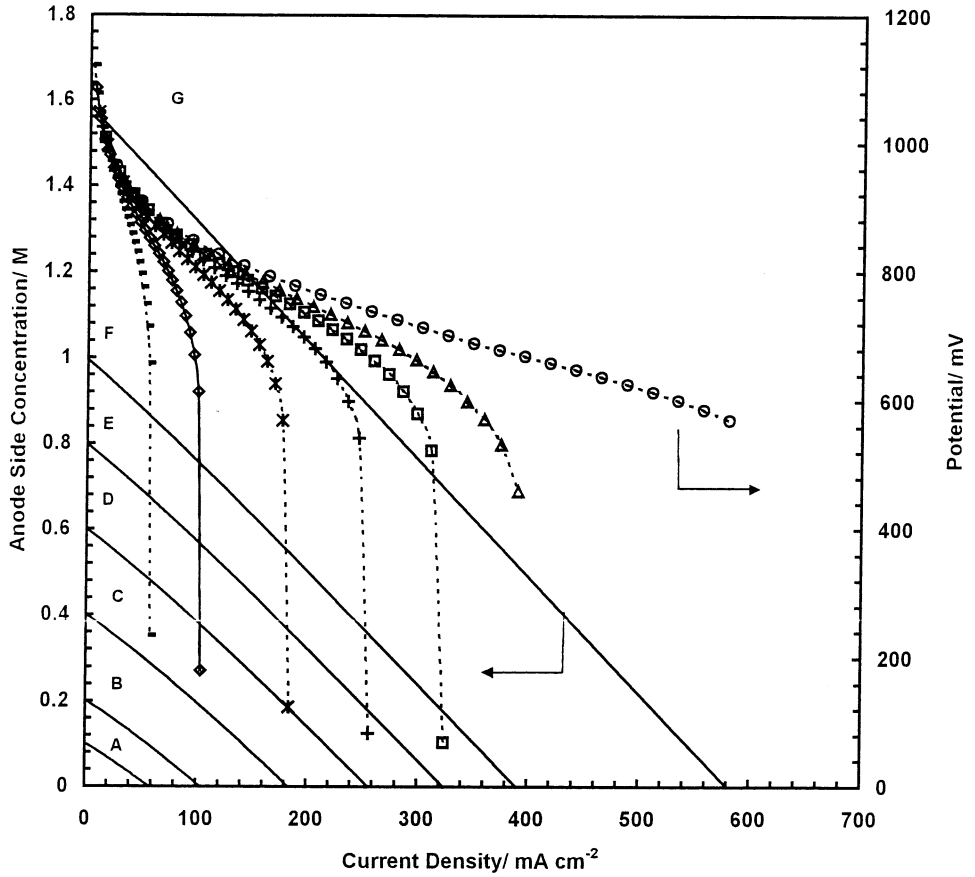

Fig. 8. Predicted variation in anode methanol concentration and anode overpotential. (a) Effect of methanol concentration. 90°C. Methanol concentration (M). A: 0.125; B: 0.25; C: 0.5; D: 0.75; E: 1.0; F: 1.25; G: 2.0. (b) Effect of temperature. 1.0 M methanol. ■: 70°C; ●: 80°C; △: 90°C.

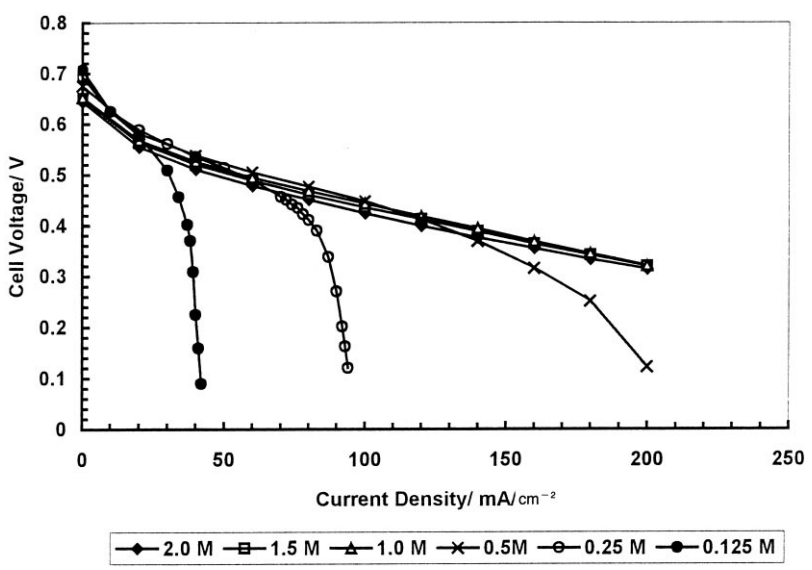

Fig. 9. Experimental DMFC cell polarisation behaviour. 90°C, 2 bar air pressure.

Fig. 8 shows the typical predicted variation in methanol concentration and anode overpotential using the above model for the anode. Estimation of the effective methanol diffusion coefficient is based on the model of the liquid voidage based on the bubble swarm calculation. The overpotential exhibits the experimental

trends seen in the cell polarisation data (Fig. 9), i.e. limiting current density is approached at high current densities and with low methanol concentrations, where the predicted concentration of methanol at the anode approaches zero. The effect of higher temperature in decreasing the overpotential for methanol oxidation and increasing the limiting current density is also predicted (Fig. 8b). The characteristic large initial drop in potential at low current densities, associated with anode polarisation is also seen. However to develop a cell polarisation curve based on the anode overpotential requires a model which conforms to the experimentally observed large difference in theoretical equilibrium potential and the measured values of the open circuit potential. This factor is influenced by complex interfacial effects at the anode and cathode catalysts and the effect of methanol crossover on the cathode.

7.2. Cell polarisation

A semi-empirical model for the open circuit voltage of the DMFC which includes the effect of methanol crossover has recently been produced [26] in the form below

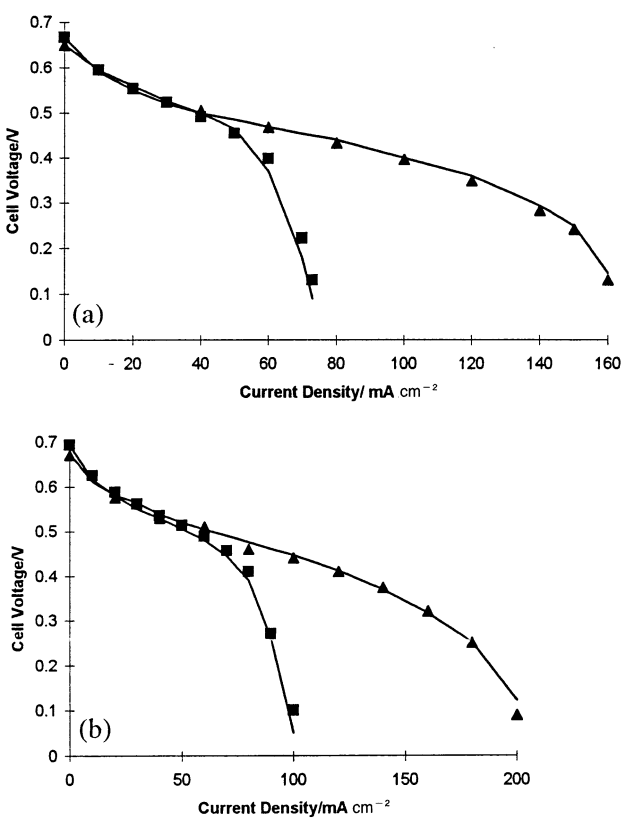

Fig. 10. Comparison between model and experimental cell polarisation data. (a) Experimental data, ▲: 0.125 M; ■: 0.375 M methanol concentration. 80°C. Solid lines model data. (b) Experimental data, ▲: 0.125 M; ■: 0.375 M methanol concentration. 70°C. Solid lines model data.

$$V_{\text{cell},0} = E^{\theta}(1-\beta) + \frac{RT}{F}\ln\left\{k_{21}^{*}(T)(c_{\text{MeOH,a}})^{1-1/\beta}\left(\frac{P_{\text{CO}_2,\text{a}}}{P^{\theta}}\right)^{-1} \times \left(\frac{P_{\text{O}_2,\text{c}}}{P^{\theta}}\right)^{3/2}\right\} \quad (31)$$

The parameter values which were determined from a least-squares fit of the experimental data, are $\beta = 0.56$ and $k_{21}^{*}(90°\text{C}) = 2.4 \times 10^{-2}$. It is assumed that the influence of methanol on the cathode mixed potential is constant and does not vary with current density, i.e. a constant overpotential due to methanol crossover exists. There is published experimental evidence to support this [12] and also we have measured concentrations of methanol in the cathode exhaust of operating fuel cells and found that they vary little with operating current density [27]. In practice a model of the effect of methanol on the mixed potential at air cathodes is required which is outside the scope of this work. An approach, under development, is to consider the simultaneous processes of oxygen reduction and methanol oxidation on the electrochemical kinetics of the cathode based on experimental data.

Overall the model for the cell potential is based on a combination of the model for the open circuit potential, the anode mass transport model, a Butler–Volmer cathode polarisation model [28] with a constant oxygen partial pressure (a large stoichiometric excess of air or oxygen is used in the experimental work) and a membrane potential drop, estimated from the published conductivity for Nafion® [29].

$$V_{\text{cell}} = V_{\text{cell},0} - IR_{\text{membrane}} - |\eta_{\text{c}} + \eta_{\text{a}}| \quad (32)$$

Fig. 10 shows a comparison between experimental cell polarisation data and model data, for 0.125 and 0.375 M methanol feed concentrations. There is generally good agreement between the two sets of data over the full range of current densities. The mass transfer limiting current behaviour is modelled satisfactorily in all cases. Although the proposed model has been validated against experimental data it does, as with most models, have a number of shortcomings. These include the need for robust models of the anode electrocatalyst layer and of the oxygen reduction catalyst in the presence of methanol. Furthermore it remains to be seen whether, or not, structural modifications and changes in material properties of the DMFC membrane electrode assembly, which influence transport properties, can be modelled satisfactorily and incorporated into an overall model of the liquid feed system. Additionally the model should also respond to variations in thermodynamic properties of, and the phase equilibrium between, aqueous methanol and carbon dioxide gas, which depend upon local conditions of temperature and pressure.

8. Conclusions

Observed limiting current densities in the DMFC have been associated with diffusion limitations in the carbon cloth and hydrodynamic limitations in the flow channel. A model of methanol mass transport in the anode side of the DMFC and through the membrane enables prediction of the concentration of methanol at the anode electrocatalyst. This model enables calculation of the anode polarisation over the full range of operating current densities and methanol concentrations. The model, in combination with a Butler–Volmer model of the cathodic reduction of oxygen gives good predictions of actual DMFC polarisation. Further improvements in the DMFC model may be realised with an improved cathode model which allow for the mixed potential at the cathode due to methanol crossover and a porous electrode diffusion model of the anode electrocatalyst layer.

Acknowledgements

The authors would like to acknowledge the following: the European Commission for a TMR Marie Curie B20 research training grant to P. Argyropoulos, Johnson Matthey Technology Centre for supplying catalyst under its loan scheme and S. Kramer for preliminary implementation of the anode model.

Appendix A. Capillary pressure model for liquid voidage

The capillary pressure model treats the porous media (carbon cloth and/or carbon diffusion layer) as a continuum with two phase flow of gas and liquid. The porous media has voidage e, which is constituted by a liquid voidage e_l and gas voidage, e_g, such that $e = e_l + e_g$.

Momentum balances for gas and liquid in the porous media are written as

$$0 = -e_g \frac{dP_g}{dz} + e_g \zeta_g g + F_g \quad (A1)$$

$$0 = -e_l \frac{dP_l}{dz} + e_l \zeta_l g + F_l \quad (A2)$$

where P_i are the local pressure of phase i, either gas g or liquid l, F_i = total drag force per unit bed volume experienced by phase i, and ζ_i is the density of phase i.

The drag forces are given by the following expressions [30]

$$F_g = -\left(\frac{A\mu_g(1-e)^2 e^{1.8}}{d^2 e_g^{2.8}} + \frac{B_{\zeta g}(1-e)e^{1.8}[U_g]}{e_g^{1.8} d}\right)U_g \quad (A3)$$

$$F_l = -\left(\frac{e-e_l^L}{e_l-e_l^L}\right)^{2.9}\left(\frac{A\mu_l(1-e)^2 e_l^2}{d^2 e^3} + \frac{B_{\zeta g}(1-e)[U_l]e_l^3}{e^3 d}\right)U_l \quad (A4)$$

where A and B are constants, μ is the viscosity, U the fluid velocity, d the average particle size of the porous media, and the limiting liquid voidage is given by

$$e_l^L = (20 + 0.9E_o^*)^{-1} \quad (A5)$$

where

$$E_o^* = \frac{\zeta_l g d^2 e^2}{\sigma(1-e)^2} \quad (A6)$$

with σ the interfacial tension.

The difference between the gas and liquid phase pressure is the capillary pressure P_c, given by

$$P_g - P_l = P_c \quad (A7)$$

The capillary pressure is related to the permeability of the porous media, k, according to the

$$P_c = \left(\frac{e}{k}\right)^{1/2} \sigma J(S_l) \quad (A8)$$

where, $J(S_l)$ is the Everett function.

This function is approximated by the following expression for a wide range of porous media [30].

$$J(S_l) = 0.48 + 0.036 \ln\left(\frac{1-S_l}{S_l}\right) \quad (A9)$$

and S_l is the saturation given by $e_g = e(1-S_l)$.

To be consistent with the Ergun equation [19], the permeability of the carbon cloth and diffusion layer is

$$\left(\frac{e}{k}\right)^{1/2} = \frac{(1-e)}{ed}\sqrt{A} \quad (A10)$$

where $A \approx 150$ and where permeability is defined in terms of Darcy's equation

$$U_g = -\frac{k}{\mu}(dP_g/dx) \quad (A11)$$

As an approximation we can assume that, because the liquid flow is small, liquid and gas flow are laminar over the thin diffusion layer, ℓ_c,a differential balance is written, by combining Eqs. (1) to (4), as

$$\left(\frac{e}{k}\right)^{1/2} \sigma J^1(e_l)\frac{de_l}{dz} = \frac{F_g}{e_g} - \frac{F_l}{e_l} \quad (A12)$$

for a vertical orientated electrode where J^1 denotes the first derivative and

$$U_g = \frac{j/6F}{\zeta_g e(1-S_l)} \quad (A13)$$

The steady state condition on this equation gives the average liquid voidage from the condition.

$$F_g/e_g = F_l/e_l \quad (A14)$$

Assuming this to be the condition at the boundary of the cloth and flow channel, i.e. away from the site of bubble generation, enables Eq. (12) above to be solved to give a spatial variation in voidage from which an average diffusion coefficient can be obtained as

$$D_{av} = \int_0^k \frac{D_{MeOH}(e_l)^{1.5}}{l_c} dz \quad (A15)$$

The liquid velocity is approximately

$$U_l = \zeta_l N'_l / 18 \quad (A16)$$

Appendix B. Notation

c	concentration
d	average size of particle in porous media
D	diffusion coefficient
e	voidage
E	electrode potential
$E°$	standard electrode potential
$E_{cell,O}$	cell voltage at open circuit
F	Faraday constant
F_i	drag coefficient
I	cell current
j	current density
j_{crit}	critical current density
j_o	exchange current density
$J(S_l)$	Leverett function
k	permeability
k_j	mass transfer coefficient
$k*$	empirical rate constant defined in Eq. (31)
k_l	mass transfer coefficient for flow channel
l	thickness of layer
m	constant defined in Eq. (2)
n	number of electrons
N	flux
N_{drag}	water flux by electroosmotic drag
N_a	flux of water associated with anode reaction
N_{d,H_2O}	water flux due to diffusion
p	partial pressure
P	pressure
P_c	capillary pressure
R	gas constant
S_l	liquid saturation
T	temperature
U	fluid velocity
V	volumetric flow
V_{cell}	cell voltage
x	mol fraction
λ	drag coefficient
σ	interfacial tension
ζ	density
ξ	effectiveness factor
α	charge transfer coefficient
β	empirical constant for methanol cross over in equation (31)
γ	empirical constant defined in equation (14)
η	overpotential
ζ_{H_2O}	density of water
μ	viscosity
z	co-ordinate direction

Subscripts

a	anode
c	carbon layer
cl	cloth
eff	effective
g	gas
l	liquid
m	membrane
MeOH	methanol
T	total
H_2O	water

Superscripts

a	anode
c	cathode
cl	carbon cloth

References

[1] G.L. Troughton, A. Hamnett, Bull. Electrochem. 7 (1991) 488.
[2] K. Scott, W.M. Taama, J. Cruickshank, J. Power Sources 65 (1997) 159.
[3] J.S. Wainwright, J.T. Weng, R.F. Savinell, M. Litt, J. Electrochem. Soc. 142 (1995) L121.
[4] Direct Methanol Fuel Cell Review Meeting, Department of Energy and Advanced Research Projects Agency, Baltimore, April 26–27, 1994.
[5] M.K. Ravikumar, A.K. Shukla, J. Electrochem. Soc. 143 (1996) 2601.
[6] S. Surampudi, S.R. Narayanan, E. Vamos, H. Frank, G. Halpert, A. LaConti, J. Kosek, G.K. SuryaPakash, G.A. Olah, J. Power Sources 47 (1994) 377.
[7] T.I. Valdez, S.R. Narayanan, H. Frank, W. Chun, Proceedings of the 12th Annual Battery Conference on Applications and Advances, 1997, p. 239.
[8] S.R. Narayana, G. Halpert, W. Chum, B. Jeffries-Nakamura, T.I. Valdez, H. Frank, S. Surampudi, Proceedings of the Power Sources Conference, Cherry Hill, NJ, USA, 1996.
[9] K.B. Prater, J. Power Sources 51 (1994) 129.
[10] M. Hogarth, P. Christensen, A. Hamnett, A.K. Shukla, J. Power Sources 55 (1995) 87.
[11] K. Scott, W.M. Taama, P. Argyropoulos, J. Appl. Electrochem. 28 (1998) 1389.

[12] P.S. Kaurenan, E. Skou, J. Electroanal. Chem. 408 (1996) 189.
[13] D. Chu, S. Gilman, J. Electrochem. Soc. 141 (1994) 1770.
[14] M.W. Verbrugge, J. Electrochem. Soc. 136 (1989) 417.
[15] J. Cruickshank, K. Scott, J. Power Sources 70 (1998) 40.
[16] K. Scott, J. Cruickshank, J. Appl. Electrochem. 28 (1998) 289.
[17] S.F. Baxter, V.S. Battaglia, R.E. White, J. Electrochem. Soc. 146 (1999) 437.
[18] R.H. Perry, D. Green, Chemical Engineers Handbook, 50th edition, McGraw Hill, New York, 1984.
[19] A.E. Scheidegger, The Physics of Flow Through Porous Media, 3rd edition, University of Toronto Press, Toronto, 1974.
[20] J.M. Coulson, J.F. Richardson, Chemical Engineering, vol. 2, 4th edition, Pergamon Press, Oxford, 1991.
[21] M.G. Fouad, G.H. Sedahmed, Electrochim. Acta 17 (1972) 665.
[22] L.J.J. Janssen, J.G. Hoogland, Electrochim. Acta 15 (1970) 1013.
[23] K. Scott, W.M. Taama, P. Argyropoulos, Electrochim. Acta 44 (1999) 3575.
[24] K. Scott, W.M. Taama, P. Argyropoulos, K. Sundmacher, J. Power Sources, accepted for publication.
[25] X. Ren, W. Henderson, S. Gottesfeld, J. Electrochem. Soc. 144 (9) (1997) L267.
[26] K. Sundmacher, K. Scott, Chem. Eng. Sci. 54 (1999) 2927.
[27] R. Reeve, P.A. Christensen, K. Scott, J. Appl. Electrochem., submitted for publication.
[28] D. Bevers, M. Wohr, K. Yasuda, K. Oguro, J. Appl. Electrochem. 27 (1997) 1254.
[29] T.E. Springer, M.S. Wilson, S. Gottesfield, J. Electrochem. Soc. 140 (1993) 3513.
[30] K. Grosser, R.G. Carbonell, S. Sundraresan, AIChE J. 34 (1988) 1851.